Environmental Engineering and Management Journal *February 2018, Vol. 17, No. 2, 293-306*
http://www.eemj.icpm.tuiasi.ro/; http://www.eemj.eu

"Gheorghe Asachi" Technical University of Iasi, Romania

ELUCIDATING THE EFFECTS OF NANOSILICA ON THE CHARACTERISTICS OF ALKALI-ACTIVATED THIN-FILM TRANSISTOR LIQUID-CRYSTAL DISPLAY WASTE GLASS

Kang Gao[1], Kae-Long Lin[2]*, Chao-Lung Hwang[3], Bui Le Anh Tuan[4], Ta-Wui Cheng[5], DeYing Wang[1]

[1]Department of Environmental and Material Engineering, Yan-Tai University, Yan-Tai, China
[2]Department of Environmental Engineering, National Ilan University, Ilan City,Taiwan
[3]Department of Construction Engineering, National Taiwan University of Science and Technology, Taipei City, Taiwan
[4]Department of Civil Engineering, Can Tho University, Can Tho City, Viet Nam
[5]Department of Materials and Mineral Resources Engineering, National Taipei University of Technology, Taipei City,Taiwan

Abstract

Thin-film transistor liquid-crystal display (TFT-LCD) waste glass can be used as a raw material for producing geopolymers, because it contains large amounts of silicon and aluminum in its amorphous structure. The setting time and compressive strength were evaluated to determine the quality of the geopolymer product with various amounts of nano-SiO_2 (0%–3%) and TFT-LCD waste glass replacement (0% - 40%). The microstructures of the samples were characterized using mercury intrusion porosimetry (MIP), Fourier transform infrared spectroscopy (FTIR), and scanning electron microscopy (SEM). The highest compressive strength and compact microstructure of the geopolymer was attained by adding 10% waste glass and 1% nano-SiO_2. The results demonstrated that adding nano-SiO_2 to the geopolymer substantially enhances compactness, improves uniformity, and greatly increases compressive strength. This work offers a low-cost route for fabricating geopolymers, because TFT-LCD waste glass can be used to partially substitute metakaolin in the composition of the geopolymer.

Key words: compressive strength, geopolymer, microstructure, nano-SiO_2, TFT-LCD waste glass

Received: June, 2013; Revised final: June, 2014; Accepted: June, 2014; Published in final edited form: February 2018

1. Introduction

In recent years, the rapid development of science and technology, resulting in the widespread use of thin-film transistor liquid-crystal display (TFT-LCD) panels in televisions, computer monitors, mobile phones, personal digital assistants, navigation systems, and projectors has generated interest in many scientists (Lin et al., 2009, 2012). TFT-LCD has many remarkable properties, such as high contrast and integration, high brightness and environmental performance, and a low cost. Thus, TFT-LCD panels can be produced in large quantities (approximately 461 million m^2 in 2014) to fully meet the demand of society, as reported by Display Search (Display Search, 2013). An estimated 9.8×10^6 tons of TFT-LCD panel glass was produced in 2013 (Lin et al., 2012). Moreover, many products were also fabricated using waste sources (Wang, 2009).

Furthermore, methods for recycling and reusing TFT-LCD waste glass have been thoroughly explored by many researchers (Amato et al., 2017; Wang, 2009). TFT-LCD waste glass was used to tune low-strength material (CLSM) to suit the technical and characteristic requirements of production including large fluidity, high permeability, and low strength and

* Author to whom all correspondence should be addressed: e-mail: kllin@niu.edu.tw; Phone: (886) 3-9357400 ext 7579; Fax: (886) 3-9364277

electrical resistivity, ushering developments in material science for using waste glass sources. TFT-LCD waste glass is used to replace a small amount of the aggregate component in fresh self-consolidated glass concrete, and is also used as a fine aggregate and pozzolanic material (Popovici et al., 2015; Wang, 2011; Wang and Huang, 2010). An estimated 69% of the TFT-LCD waste glass in Taiwan has been obtained from recycling processes. The rapid development of industry and qualitative improvement of life has resulted in a substantial increase in the amount of waste glass being discarded into the environment. Nevertheless, only a small amount of such waste has been reused or recycled, creating a serious threat to the ecosystem (Park et al., 2004). In addition, abundant waste electrical and electronic equipment (WEEE) are also discharged into the environment every year. It is thus challenging to process and substantially reduce the amount of waste released into the environment (Lin et al., 2012).

To overcome the challenges in ensuring a clean environment and improving the quality of life, TFT-LCD waste glass can be disposed of using several methods, and it can be reused in various applications. TFT-LCD waste glass is used as a component in geopolymer mixtures. Herein, geopolymer is a novel type of high-performance cement, developed by Joseph Davidovits in the 1970s (Alaa, 2013; Davidovits, 1991). This material is synthesized by alkaline or silicate activation of alumina and silica sources, acting as a reducing agent for geopolymerization (Alaa, 2013; Khale and Chaudhary, 2007). Polymerization occurs in the presence of an alkali hydroxide and a silicate solution under highly alkaline conditions, generating free SiO_4 and AlO_4 tetrahedral ions in the solution. These ions can be alternatively linked to form amorphous geopolymer structures through an electronic transference between positive ions (e.g. K^+, Na^+) and negative ions (e.g., oxygen) (Duxson et al., 2007). Moreover, TFT-LCD waste glass has been used as a high-quality glass-ceramic material, eco-brick, and ceramic tile, as previously reported by Lin (2007a, 2007b).

Geopolymeric materials are attractive to scientists because of their excellent and promising properties (i.e., high compressive strength, low permeability, prevention of corrosion in an acidic medium, and a substantial decrease in the mobility of most heavy metal ions in the geopolymer structure) (Davidovits, 1989; van Jaarsveld et al., 1997; Zhang et al., 2010). Geopolymers can be more easily fabricated than Portland cement, and do not require high temperatures for calcining or sintering. Therefore, the polymerization reaction can be conducted at room temperature, generating high-quality geopolymer products that can be used as promising green building materials, because they reduce toxic waste in the environment, exhibit high temperature-resistance (Álvarez-Ayuso et al., 2008), and emit only a small amount of CO_2, with a negligible presence of NO_x, SO_x, or CO (Komnitsas, 2011). The nature and characteristics of the raw material determine the structure of the geopolymer (i.e. its microstructure, properties of the gel formed, and support of inorganic polymers). Thus, not only kaolinite and other clays have been used as raw materials for fabricating geopolymers, but also various wastes have been used (e.g. fly ash and slag) (Zaharaki et al., 2010).

Nanomaterials play a crucial role in the development of materials science. Nanomaterials are used to develop advanced nanodevices and green materials with superior properties for construction. The size of nanoparticles is in the range from 1 to 100 nm, creating substantial changes to the volume and surface area of the material. Nanoparticles can also be used to develop high-performance polymers (Yang et al., 2001), to fabricate novel materials with excellent properties, and to improve the function and characterization of conventional materials by using nanocoatings, high-strength structural materials, macromolecular-based nanocomposites, magnetic materials, optical materials, and biomaterials (Zheng et al., 2005). However, studies on geopolymers that incorporate nanoparticles to improve their physical and mechanical properties are scarce.

In this study, we investigated the feasibility of using TFT-LCD waste glass as a raw material, and determined the optimal addition of nano-SiO_2 with various amounts and reaction times for producing a geopolymer with enhanced physical and mechanical properties. The resulting material not only exhibited an increased compressive strength, but also an enhanced stability.

2. Materials and methods

2.1. Materials

The TFT-LCD waste glass (66.92% SiO_2, 16.92% Al_2O_3, and 13% CaO) was taken from the TFT-LCD manufacturing plant in Taiwan. Raw TFT-LCD waste glass was milled using chrome steel balls to make its fineness approximately ~300 m^2/kg. Sodium silicate (Na_2SiO_3) solution was produced in Taiwan containing 29.5% SiO_2, 9.1% Na_2O, 61.4% H_2O, and Ms (SiO_2/Na_2O) = 3.4. Sodium hydroxide (NaOH; 99%) was purchased from Acros. Nano-SiO_2 (99.9% of SiO_2 content, average particle size ~10 nm, and specific surface area ~670 m^2/g) was synthesized in previous study (Gao et al., 2014). Metakaolin (specific gravities ~1.66, pH value 5.74, and the fineness of 780 m^2/kg) containing 59.6% SiO_2 and 38% Al_2O_3 was obtained from kaolin (specific gravities ~1.74, pH value 6.52, and the fineness of 778 m^2/kg) calcined at 650 °C for 3 h (Gao et al., 2014). The chemical composition of raw materials was determined by X-ray fluorescence.

2.2. Sample preparation

NaOH and distilled water were mixed with a Na_2SiO_3 solution and allowed to cool to room

temperature. The SiO_2/Na_2O ratio was 1.50 and solid-to-liquid ratio was 1.03. With continuous stirring, nano-SiO_2 (0%, 1%, 2% and 3%), and TFT-LCD waste glass (0%, 10%, 20%, 30% and 40%), were added into the alkali activator.

The alkali activator solution was prepared 24 h before using to ensure the activator component was mixed uniformly. Table 1 shows the mixture proportions. A mechanical mixer was used to mix the activator solution, metakaolin and TFT-LCD waste glass for ~6 min. The fresh paste was then rapidly poured into plastic molds (5×5×5 cm). All specimens were placed into an oven at 80°C for 24 h, relative humidity (RH) ~30%. And after that, all samples were maintained at 30°C, RH (30%). The compressive strength and the microstructure performance of specimens were tested after 1, 7, 14, 28 and 60 days.

2.3. Analytical methods

1. Setting Time: Testing method determine the setting time of pastes by means of the Vicat needle according to the ASTM C191.

2. Compressive strength: Compressive strength tests were performed after 1, 7, 14, 28 and 60 days using a 50 mm × 50 mm × 50 mm cubic specimen, according to ASTM C109.

3. Mercury intrusion porosimetry (MIP): A Quantachrome Autoscan Mercury Intrusion Porosimeter was used, with intrusion pressures up to 60,000 psi. By using the Washburn equation, $p = -\frac{2\gamma\cos\theta}{r}$, the pore volume (V) and the corresponding radius (r) was synchronous plotted by an X-T plotter, under the assumption that mercury wetting angle was θ=140°. In this equation, p, γ, r, θ, stand for the applied pressure, surface tension, pore radius and wetting angle, respectively.

4. Chemical composition: X-ray fluorescence (XRF) analysis was performed using an automated RIX 2000 spectrometer. Specimens were prepared for XRF analysis by mixing 0.4 g of sample and 4 g of 100 Spectroflux at a dilute ratio of 1:10. The homogeneous mixtures were placed in Pt–Au crucibles before being heated for 1 h at 1000°C in an electric furnace. The homogeneous melted sample was recast into glass beads 2 mm thick and 32 mm in diameter.

5. Fourier transform infrared spectroscopy (FTIR): FTIR was carried out on samples using a Perkin Elmer FTIR Spectrum L16000A Spectrometer and the KBr pellet technique (1 mg powder of sample was mixed with 150 mg KBr).

6. Scanning electron microscope (SEM): The microstructure of geopolymer was observed using an electron beam from a Tescan Vega TS5136MM. For SEM analysis, samples were taken from specimens fractured during compression testing and mounted by epoxy resin, polished and sputter coated with gold-palladium alloy. All samples were vacuum-dried overnight prior to testing for SEM using a beam at 10 KeV.

3. Results and discussions

3.1. Setting time

Fig. 1 and Table 2 show the initial and final setting times of a waste glass-metakaolin-based geopolymer with various amounts of nano-SiO_2. The setting time was substantially increased by increasing the replacement level of waste glass, and decreased by increasing the amount of nano-SiO_2 added.

Table 1. Ratios of material in the mixture

Nano-SiO_2 addition (%)	***Waste glass replacement level (%)***	***Mix proportion by weight (g)***					
		Metakaolin	***Waste glass***	***Nano-SiO_2***	***Na_2SiO_3***	***NaOH***	***H_2O***
0	0	1000	0	0	862.7	124.5	228.5
	10	900	100	0	862.7	124.5	228.5
	20	800	200	0	862.7	124.5	228.5
	30	700	300	0	862.7	124.5	228.5
	40	600	400	0	862.7	124.5	228.5
1	0	1000	0	10	862.7	124.5	228.5
	10	900	100	10	862.7	124.5	228.5
	20	800	200	10	862.7	124.5	228.5
	30	700	300	10	862.7	124.5	228.5
	40	600	400	10	862.7	124.5	228.5
2	0	1000	0	20	862.7	124.5	228.5
	10	900	100	20	862.7	124.5	228.5
	20	800	200	20	862.7	124.5	228.5
	30	700	300	20	862.7	124.5	228.5
	40	600	400	20	862.7	124.5	228.5
3	0	1000	0	30	862.7	124.5	228.5
	10	900	100	30	862.7	124.5	228.5
	20	800	200	30	862.7	124.5	228.5
	30	700	300	30	862.7	124.5	228.5
	40	600	400	30	862.7	124.5	228.5

Table 2. Setting time of waste glass-metakaolin-based geopolymer with various nano-SiO_2 additions

Nano-SiO_2 Addition (%)	*Waste Glass Replacement Level (%)*	*Initial Setting (min)*	*Final Setting (min)*
0	0	300	345
	10	320	360
	20	349	390
	30	360	405
	40	390	435
1	0	283	330
	10	289	345
	20	324	375
	30	330	390
	40	360	405
2	0	240	285
	10	270	315
	20	285	330
	30	305	360
	40	342	390
3	0	210	270
	10	250	300
	20	262	315
	30	300	345
	40	324	375

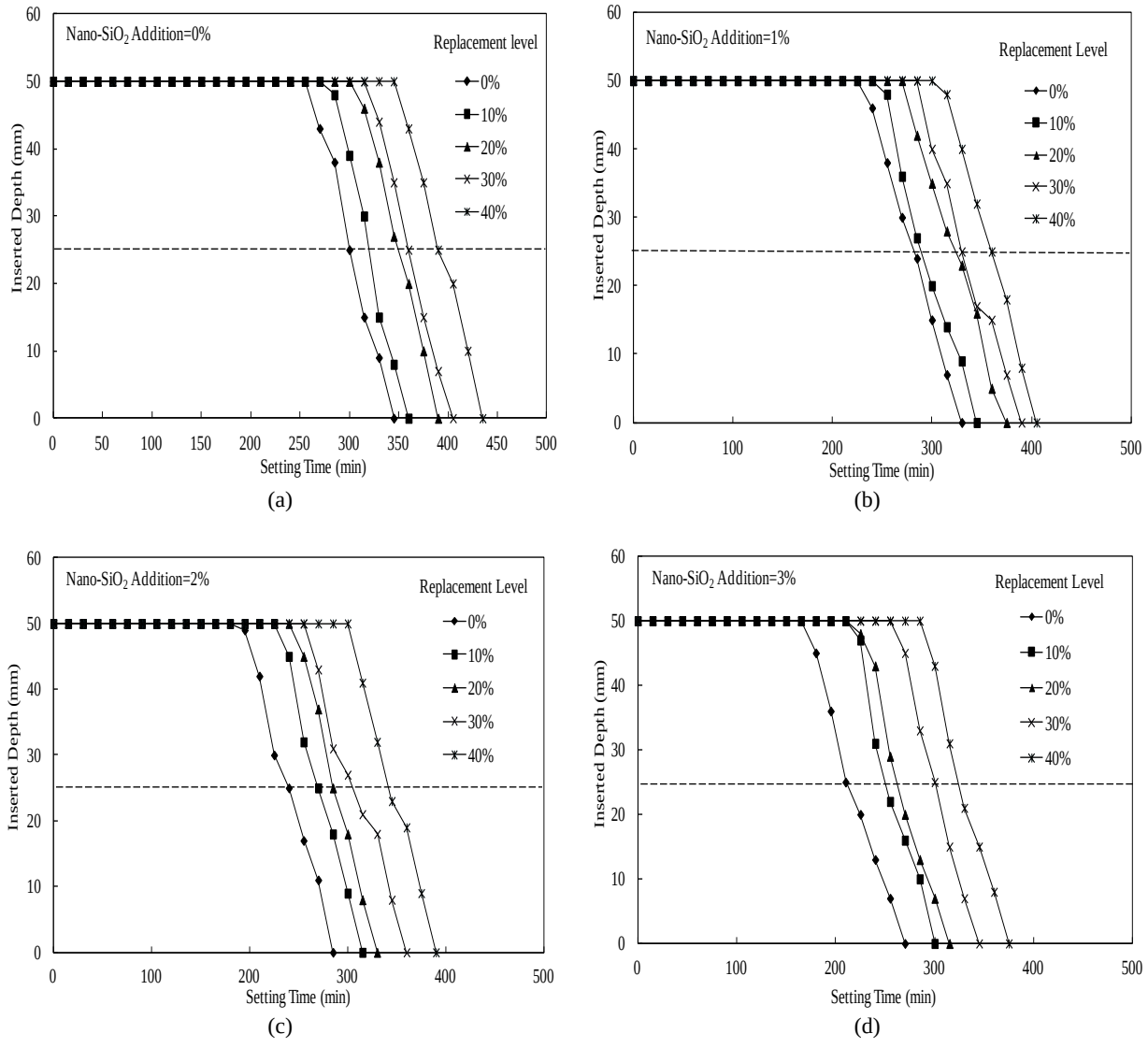

Fig. 1. Initial and final setting time of waste glass-metakaolin-based geopolymer with various nano-SiO_2 additions: (a) NS Addition=0%, (b) NS Addition=1%, (c) NS Addition=2% and (d) NS Addition=3%

The initial setting times of the waste glass-metakaolin-based geopolymer samples with a 0%, 10%, 20%, 30%, and 40% TFT-LCD waste glass replacement were 300, 320, 349, 360, and 390 min, and the final setting times were 345, 360, 390, 405, and 435 min, respectively. The setting time gradually increased with an increase in the amount of waste glass, indicating that glass was diluted in the system. Moreover, adding nano-SiO_2 shortened the initial and final setting times, suggesting that the unique nano-SiO_2 surfaces were affected (i.e., resulting in a small particle size, high surface energy, and large surface area), generating an accelerated reaction rate for the system (Lin et al., 2008; Zhang et al., 2012).

3.2. Compressive strength

Fig. 2 shows the compressive strength of the waste glass-metakaolin-based geopolymer with various amounts of nano-SiO_2. These results demonstrated that the compressive strength of geopolymers could be increased by increasing the curing time. Herein, substantial differences in the compressive strength development of geopolymers were observed, as a result of the addition of various amounts of nano-SiO_2 and TFT-LCD waste glass. In particular, the highest compressive strength of the geopolymer product was obtained by adding 1% nano-SiO_2 and 10% TFT-LCD waste glass.

The compressive strength of the specimens substantially increased after adding nano-SiO_2, and the optimal amount of nano-SiO_2 was 1%. Diverse unsaturated and hydroxy bonds exist on the nano-SiO_2 surface, which are an in an active and high free-energy state, increasing the reaction rate and degree of polymerization. In addition, nanoparticles could be filled into the paste pore, greatly increasing the compressive strength of the geopolymer. By contrast, when too many nanoparticles are added to the geopolymer mixture, a considerable amount of nanoparticles is left unreacted, resulting in agglomeration of the nano-SiO_2 particles. This substantially reduces the compressive strength of the geopolymer, and results in structural defects because of the large dispersion attained at a high concentration of nanoparticles (Wang et al., 2005).

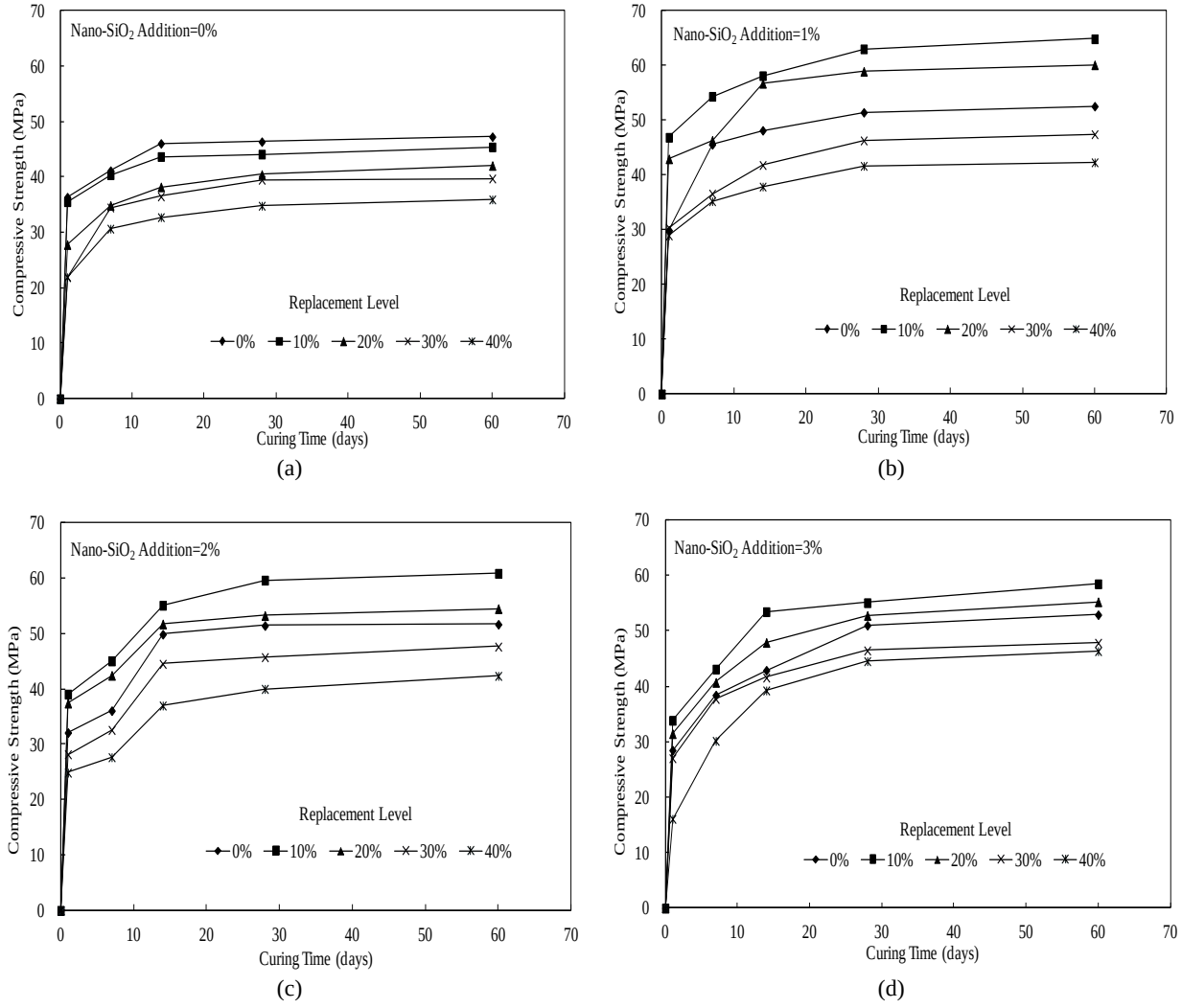

Fig. 2. Compressive strength of waste glass-metakaolin-based geopolymer with various nano-SiO_2 additions: (a) NS Addition=0%, (b) NS Addition=1%, (c) NS Addition=2% and (d) NS Addition=3%

The raw materials of a geopolymer need to be soluble in alkaline solutions, thus, the amorphous type is the optimal choice. The main components of the amorphous TFT-LCD waste glass are SiO_2 and Al_2O_3, which are typically formed by the alkali activation of aluminum silicate. A geopolymer containing 10% or 20% of TFT-LCD waste glass releases more silicon and aluminum ions than does a geopolymer not containing waste glass. The formation of AlO_4 and SiO_4 tetrahedral fragments increases, greatly affecting the evolution of the compressive strength of the system (Xu and van Deventer, 2000). The compressive strength values of the geopolymer containing 1% of nano-SiO_2 and 0%, 10%, 20%, 30%, and 40% of TFT-LCD waste glass were 52, 65, 60, 47, and 42 MPa, respectively, after 60 days of curing. This result indicated that the compressive strength of the geopolymer was substantially decreased when the amount of TFT-LCD waste glass increased to 40%. Because an excess of TFT-LCD waste glass provides more silica and less aluminum, the synthesis of the aluminosilicate becomes difficult. Therefore, the optimal amount of waste glass in the geopolymer was 10%, creating a high-quality geopolymer product with high compressive strength.

3.3. MIP results

Polymerization generates geopolymer hydration products. These products increase with an increase in the reaction degree, filling holes and making structures denser. According to the IUPAC pore radius classification, pores are classified as micropores, mecropores, macropores, and air voids or cracks. Micropore, mecropore, macropore, and void or crack apertures are < 1 nm, 1 to 25 nm, 25 to 5000 nm, and 5000 to 50,000 nm, respectively (Kong et al., 2007). The MIP technique enables an understanding of the effects of the various replacement levels of TFT-LCD waste glass and nano-SiO_2 additions on the connectivity and capacity of the geopolymer pore structure.

Figs. 3 and 4 show the cumulative pore volumes of the TFT-LCD waste glass-metakaolin-based geopolymer with various amounts of nano-SiO_2 at 28 days of curing.

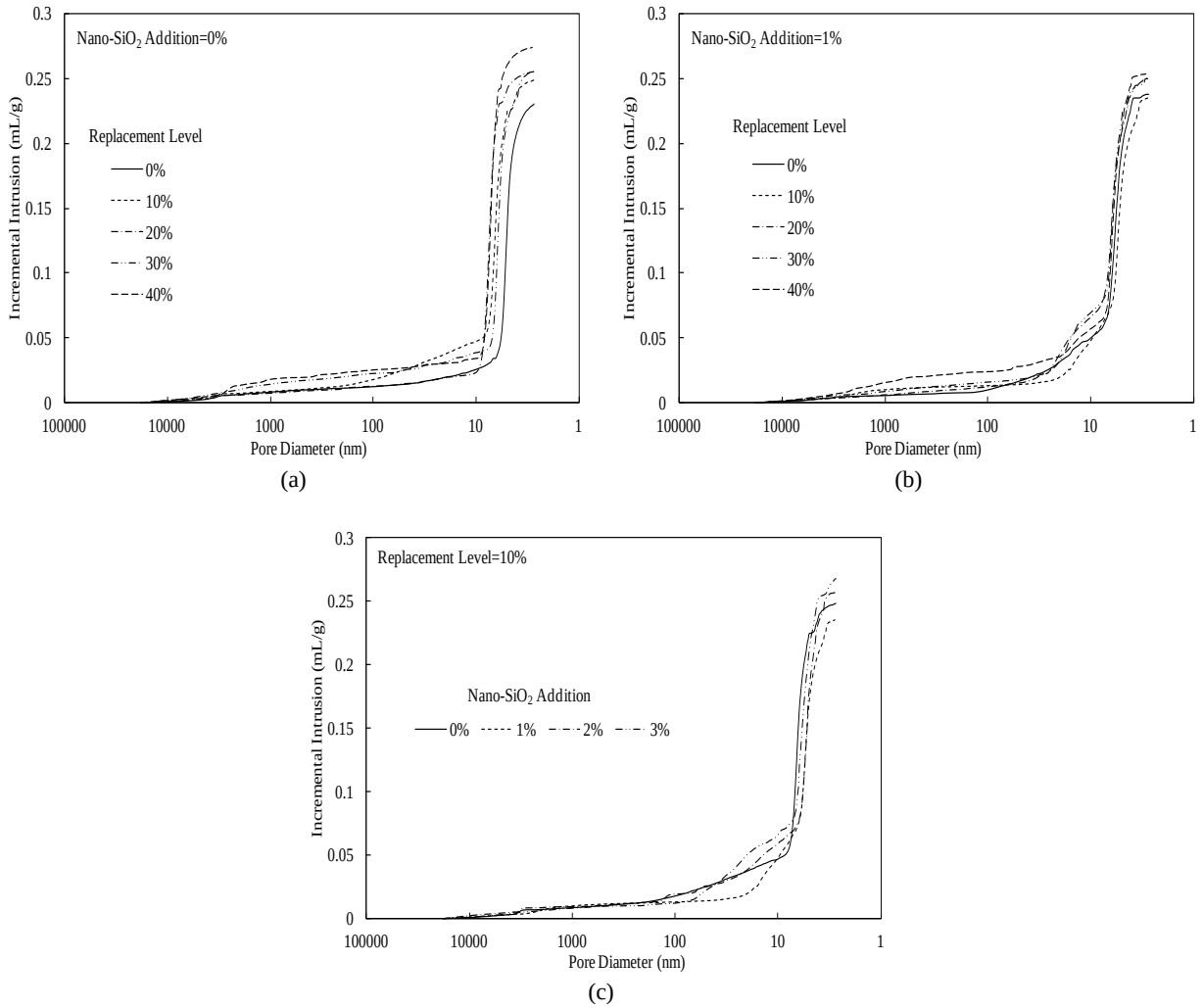

Fig. 3. Cumulative pore volume of waste glass-metakaolin-based geopolymer with various nano-SiO_2 additions (Curing time=28 days): (a) nano-SiO_2 addition=0%, (b) nano-SiO_2 addition=1% and (c) TFT-LCD waste glass replacement level= 10%

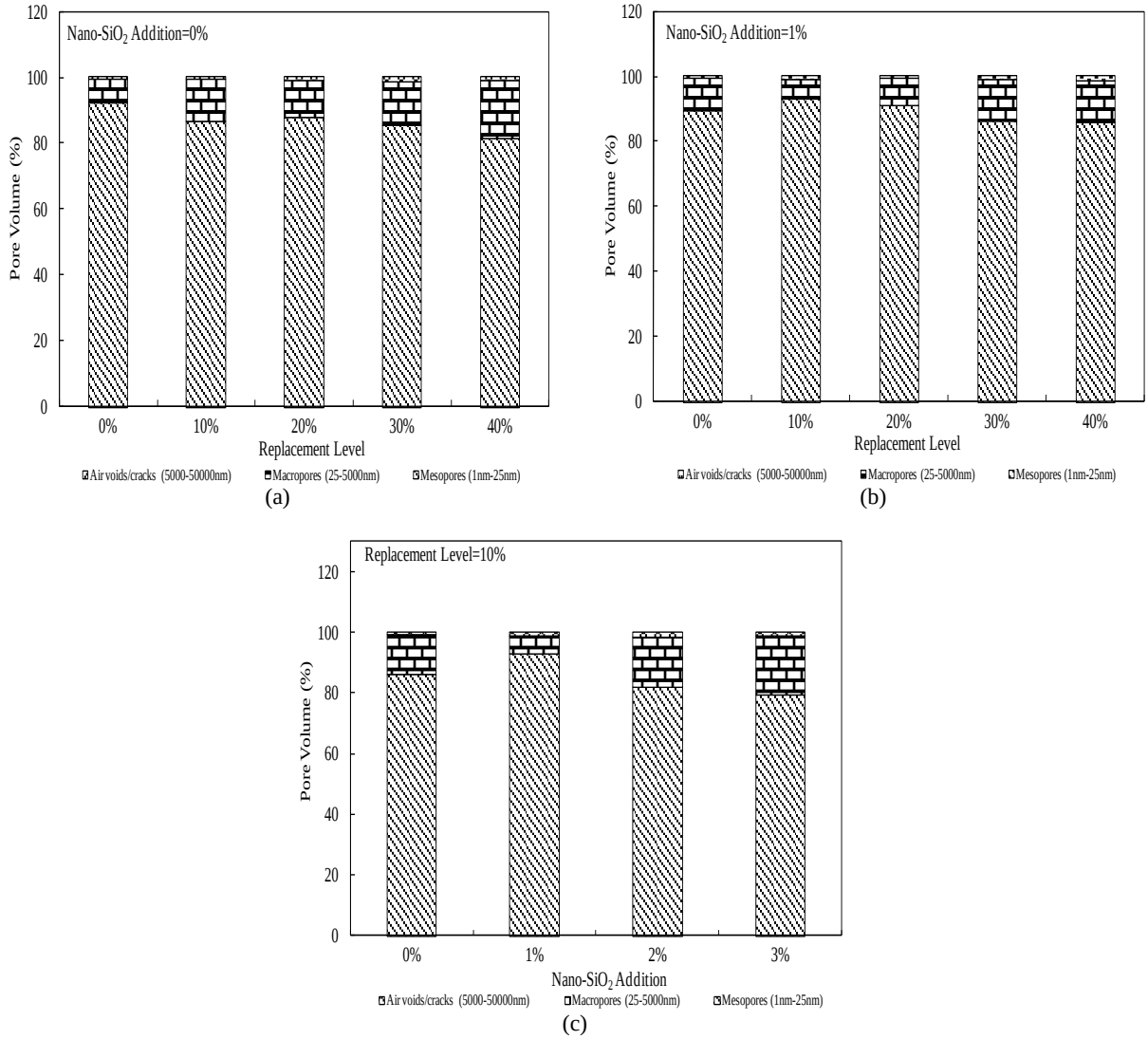

Fig. 4. Percentage of pore volume of waste glass-metakaolin-based geopolymer with various nano-SiO_2 additions (Curing time=28 days): (a) nano-SiO_2 addition=0%, (b) nano-SiO_2 addition=1% and (c) TFT-LCD waste glass replacement level= 10%

The cumulative pore volume of the waste glass-metakaolin-based geopolymer was distributed in a wide range from 10 to 100 nm, and was larger than that of the original geopolymers. After adding nano-SiO_2, the cumulative pore volume of the samples substantially decreased, and the pore distribution became increasingly narrow. When the replacement level of the waste glass was 10% and 1% of nano-SiO_2 was added, the cumulative pore volume became increasingly dense. As the cumulative pore volume decreased, the paste structure tended toward densification. This was consistent with the compressive strength results.

Figs. 5 and 6 display the pore volume percentage of the TFT-LCD waste glass-metakaolin-based geopolymer with various amounts of nano-SiO_2 after 60 days of curing. Mesopores were observed in the aluminosilicate gel network. Macropores transformed into mesopores by the polycondensation of hydrated gels and the effects of nano-SiO_2. The literature indicated that pores larger than 200 nm in geopolymer paste are probably associated with interfacial spaces between the raw material and geopolymer gel (Rodríguez et al., 2013). After adding 1% nano-SiO_2 to metakaolin-based geopolymer and replacement level of 10% TFT-LCD waste glass, the sample structure tended toward densification after 60 days of curing.

3.4. FTIR analysis

Figs. 7 and 8 present the FTIR spectra of the waste glass-metakaolin-based geopolymer substituted with 0%–40% TFT-LCD waste glass after 28 and 60 days of curing, respectively. The FTIR spectrum of the geopolymer exhibited a distinct intensity band between 1300 and 900 cm^{-1}, which was associated with the Si-O-T asymmetric stretching vibration resulting from the TO_4 reorganization that took place during synthesis (Zaharaki et al., 2010). The apparent band at approximately 470 cm^{-1} was attributed to Si-O-Si bending. The peak between 900 and 1300 cm^{-1} is often used to determine the degree of polymerization because its bonding is clearer than that of Si-O-Si bonding (Chindaprasirt et al., 2009). The peak adsorption at 700 cm^{-1} was assigned to Si-O-Al

bonding, proving that the main geopolymer structure was generated after a reaction occurred between silicon aluminates and a highly alkaline solution, which formed the Si-O-Al bonding. A weak Al-O-T binding band was observed between 540 and 555 cm^{-1}. Bands near 800 cm^{-1} were observed during the characterization of the initial metakaolin (corresponding to an Al (IV)-O vibration band) (Granizo et al., 2000).

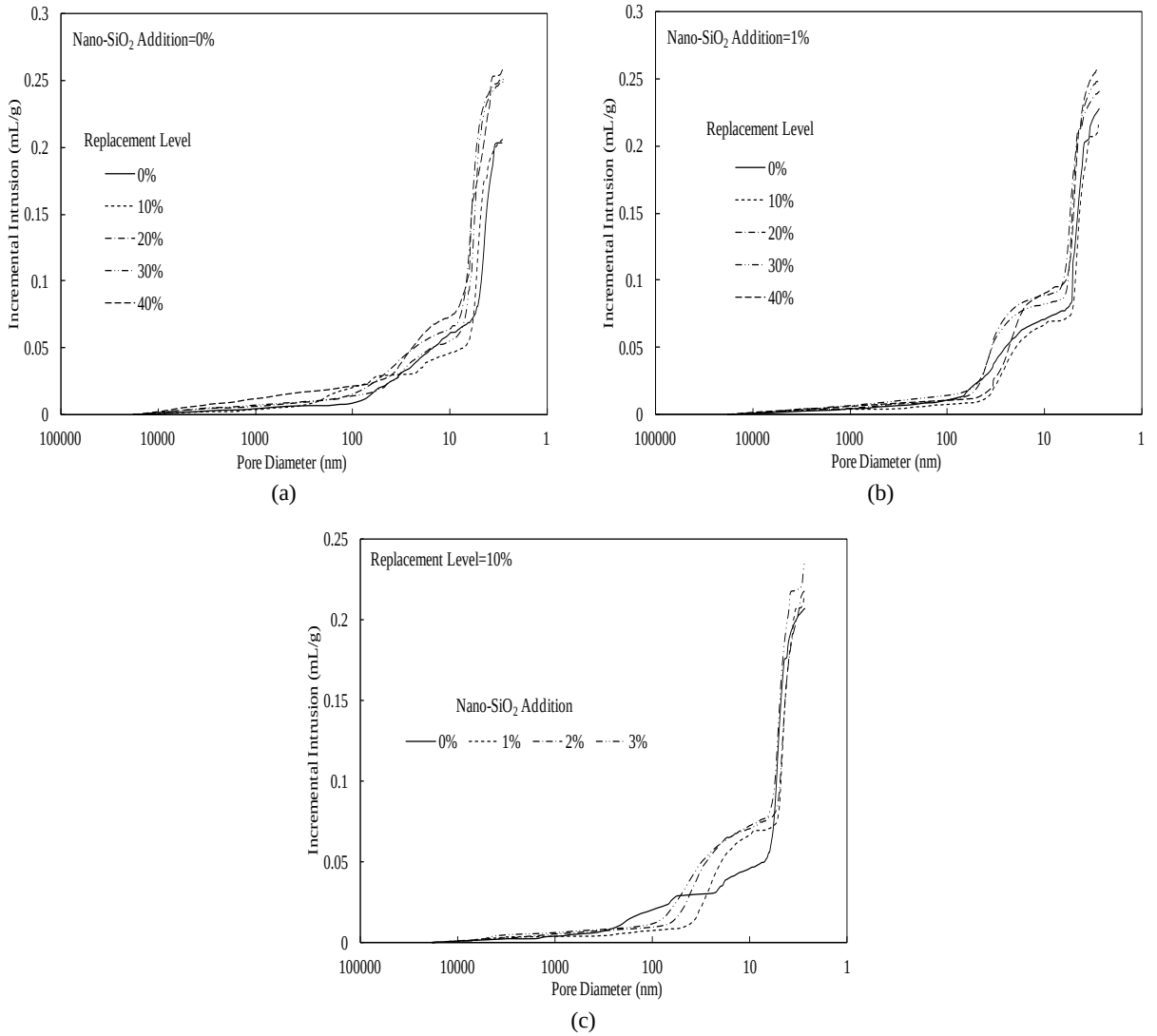

Fig. 5. Cumulative pore volume of waste glass-metakaolin-based geopolymer with various nano-SiO_2 additions (Curing time = 60 days): (a) nano-SiO_2 addition=0%, (b) nano-SiO_2 addition=1% and (c) TFT-LCD waste glass replacement level= 10%

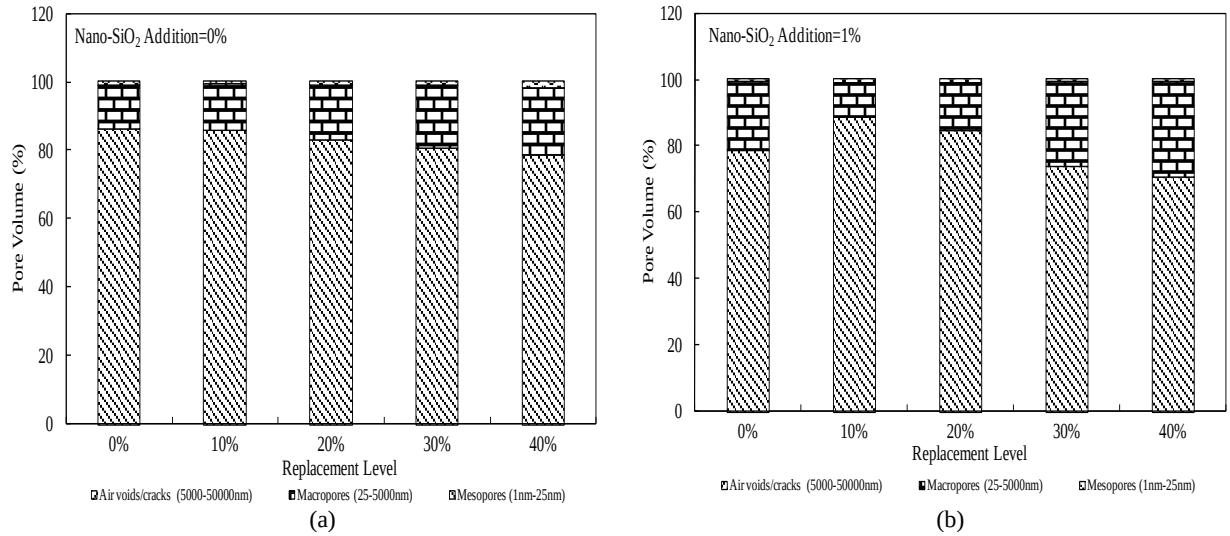

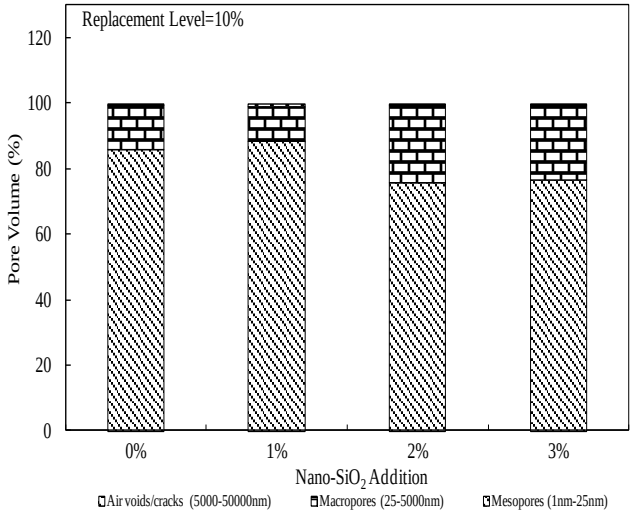

(c)

Fig. 6. Percentage of pore volume of waste glass-metakaolin-based geopolymer with various nano-SiO_2 additions (Curing time=60 days): (a) nano-SiO_2 addition=0%, (b) nano-SiO_2 addition=1% and (c)TFT-LCD waste glass replacement level= 10%

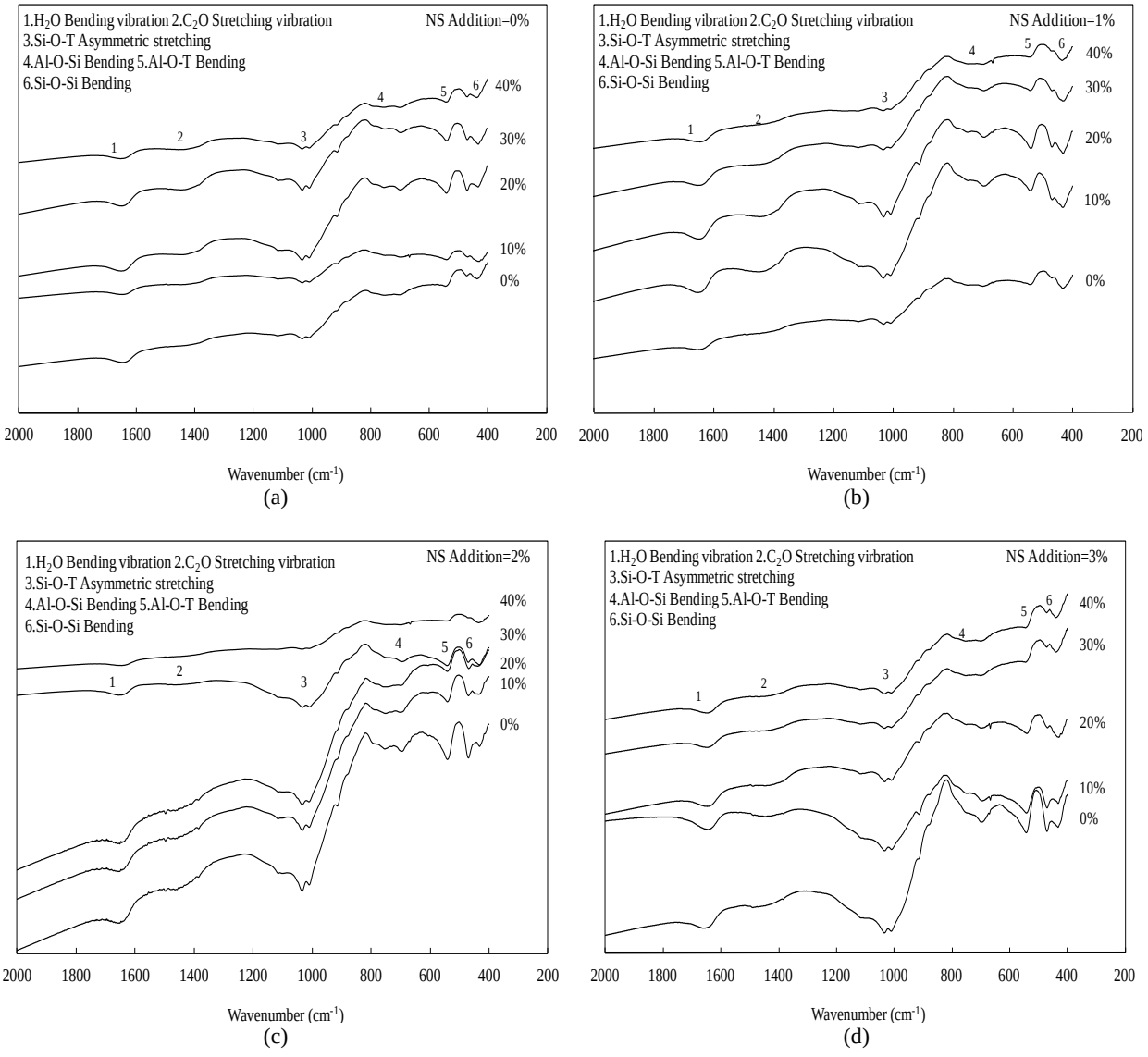

Fig. 7. FTIR spectra of waste glass-metakaolin-based geopolymer with different additions of nano-SiO_2 (Curing Time =28 days): (a) NS Addition=0%, (b) NS Addition=1%, (c) NS Addition=2% and (d) NS Addition=3%

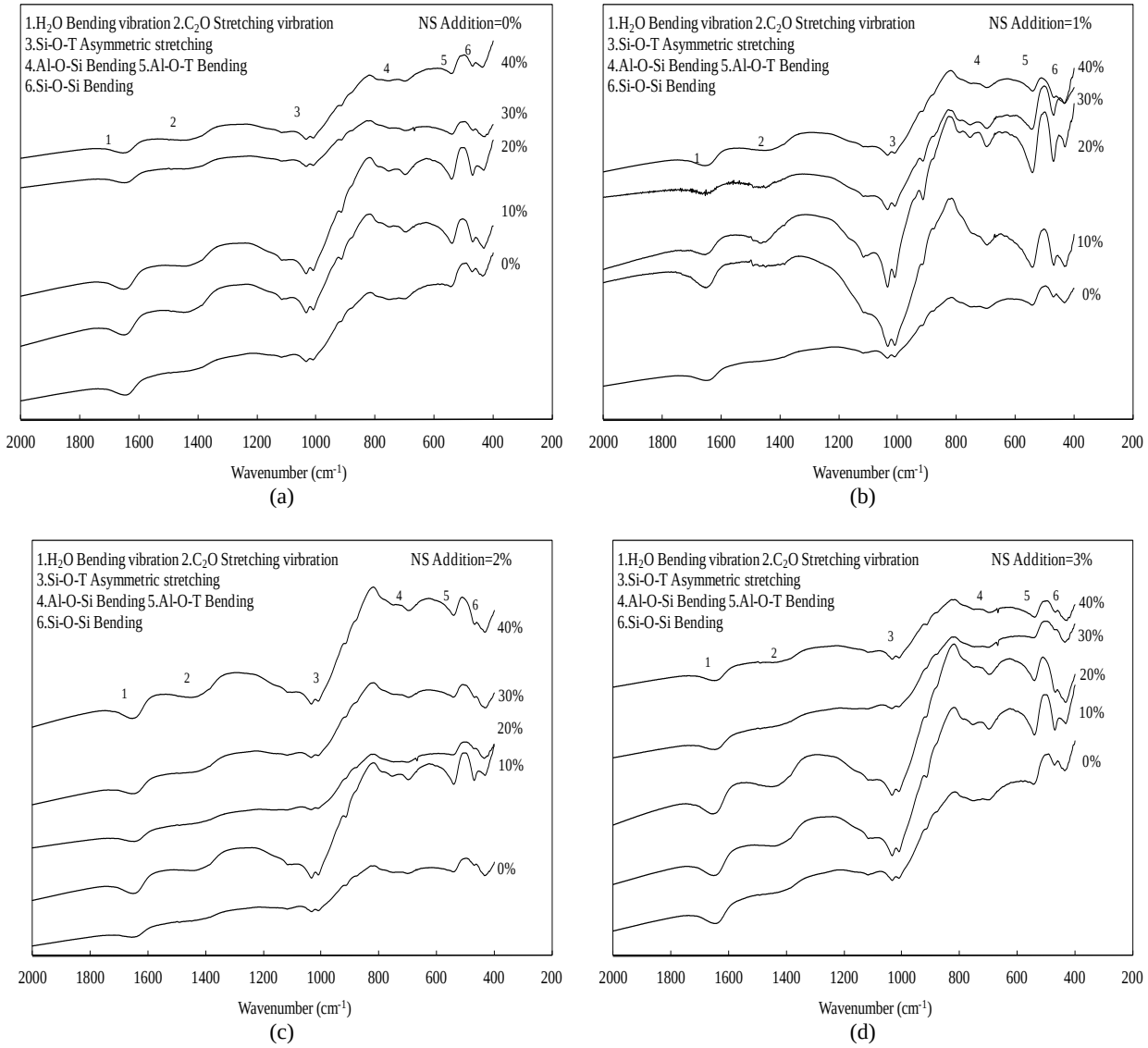

Fig. 8. FTIR spectra of waste glass-metakaolin-based geopolymer with different additions of nano-SiO_2 (Curing Time =60 days) : (a) NS Addition=0%, (b) NS Addition=1%, (c) NS Addition=2% and (d) NS Addition=3%

In addition, the peaks at 1650 and 1655 cm^{-1} corresponded to OH vibrations. These peaks indicated the presence of weak H_2O bonds absorbed on the surface or caught in the cavities of the structure (Heah et al., 2012). The band at approximately 1460 cm^{-1} is related to carbonate formation as a result of the reaction between an alkali metal hydroxide and atmospheric CO_2 (Andini et al., 2008).

3.5. SEM observation

A scanning electron microscope (SEM) was used to observe the morphological features of the geopolymers with various degrees of reaction and different ratios of activation medium. Micrographs were taken to analyze the microstructural evolution of the geopolymers. A dense appearance reflected the advance of the geopolymerization reaction of samples activated with an alkaline solution (Heah et al., 2012). Figs. 9–12 display the microstructures of the waste glass-metakaolin-based geopolymer with 0%–40% TFT-LCD waste glass after 28 and 60 days of curing. All specimens were heterogeneous, had large particle sizes, and their pores were embedded in the matrix after 60 days of curing. In addition, unreacted and flaked metakaolin or waste glass particles were clearly observed with a 40% replacement level of waste glass after 60 days of curing (Fig. 11(e)).

The geopolymer products formed loose structures and large pores. Nevertheless, the structure of the TFT-LCD waste glass-metakaolin-based geopolymer with 10% or 20% waste glass was compact with few unreacted particles, generating a geopolymer structure with high compressive strength. Furthermore, the metakaolin-based geopolymer containing 10% of waste glass exhibited high compressive strength.

The structures of geopolymers with nano-SiO_2 added into the alkali-activated solution are displayed in Fig. 12. A high degree of interaction between the gel and the waste glass particles in the matrix prepared with nanosilica-added activators was observed.

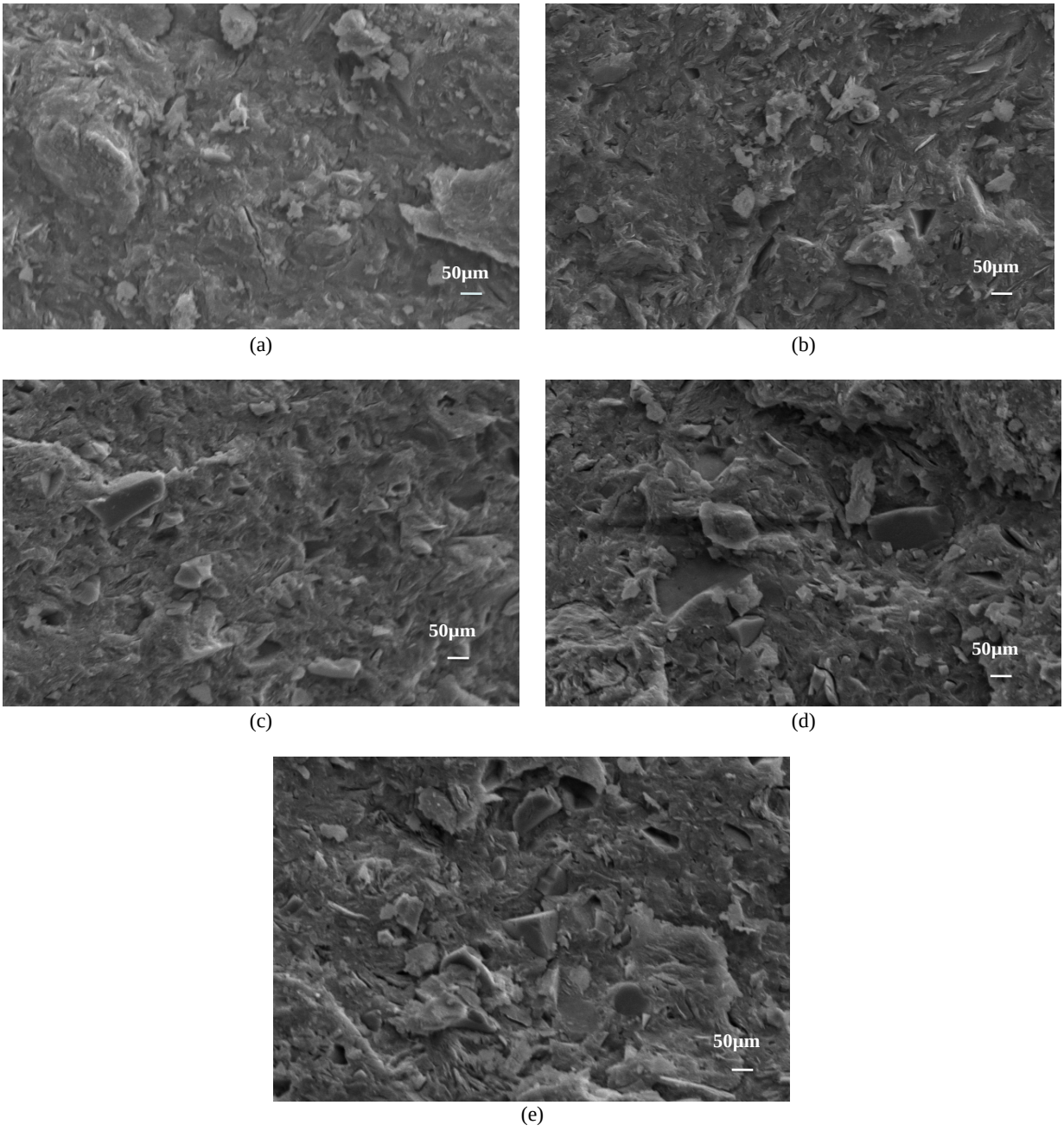

Fig. 9. SEM photographs of waste glass-metakaolin-based geopolymer with different replacement levels of TFT-LCD waste glass (Curing time=28 day): (a) Replacement Level =0%, (b) Replacement Level =10%, (c) Replacement Level = 20%, (d) Replacement Level = 30%, (e) Replacement Level = 40%

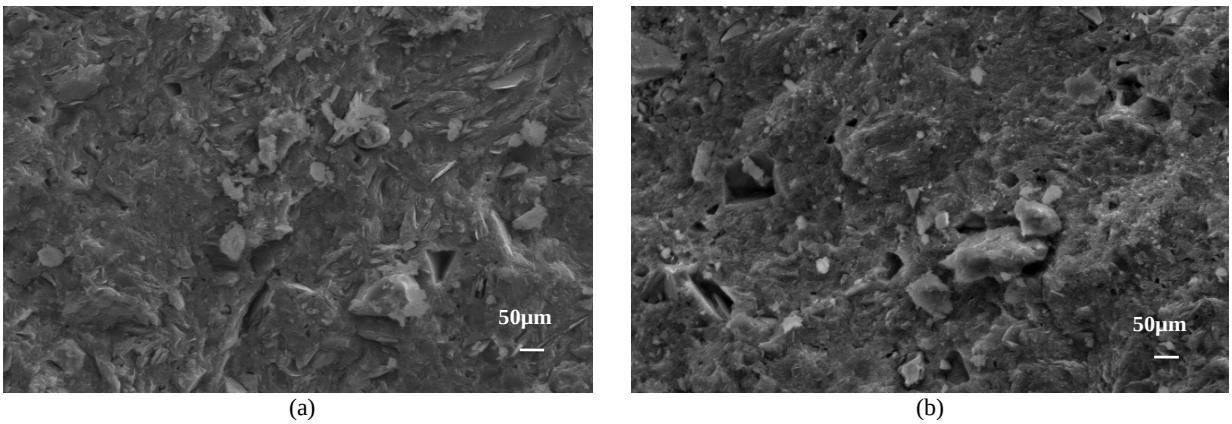

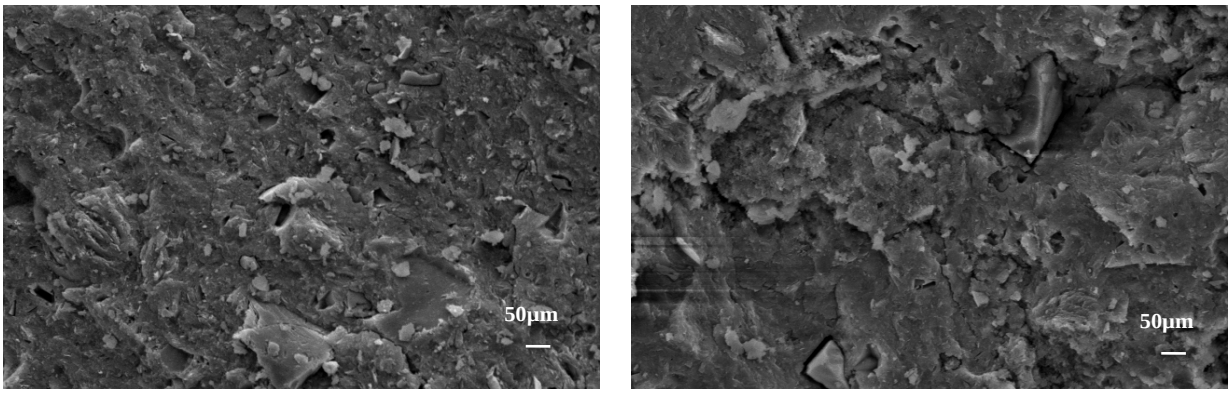

(c) (d)

Fig. 10. SEM photographs of 10% waste glass-metakaolin-based geopolymer with various nano-SiO_2 (NS) additions (Curing time=28 days): (a) NS Addition=0%, (b) NS Addition=1%, (c) NS Addition=2% and (d) NS Addition=3%

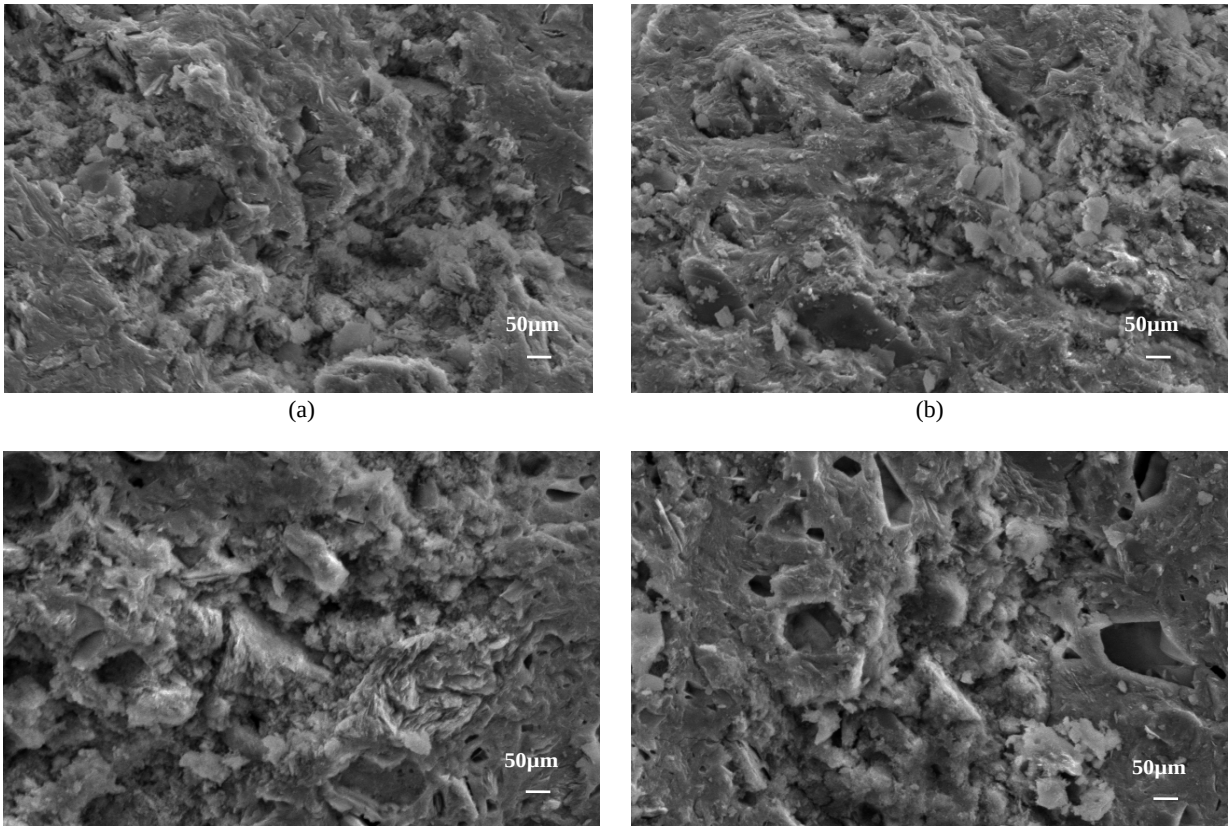

(a) (b)

(c) (d)

(e)

Fig. 11. SEM photographs of waste glass-metakaolin-based geopolymer with different replacement levels of TFT-LCD waste glass (Curing time=60 days): (a) Replacement Level=0%, (b) Replacement Level=10%, (c) Replacement Level=20%, (d) Replacement Level= 30% and (e) Replacement Level= 40%

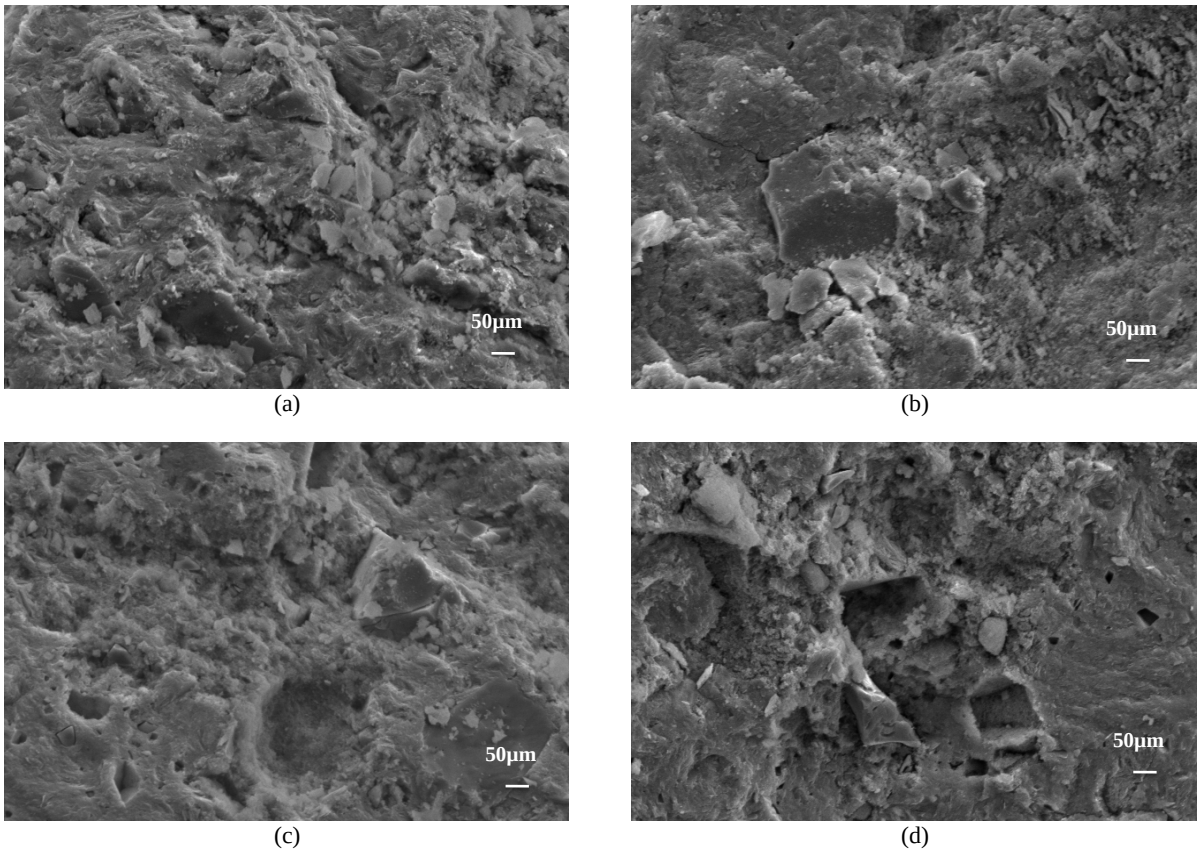

Fig. 12. SEM photographs of 10% waste glass-metakaolin-based geopolymer with various nano-SiO_2 (NS) additions (Curing time=60 days): (a) NS Addition=0%, (b) NS Addition=1%, (c) NS Addition=2% and (d)NS Addition=3%

The result was consistent with Erich, who reported that the binder compound with nanosilica-derived activators produced a material with a high reaction degree and low permeability (Rodríguez et al., 2013). Furthermore, the structure of the samples with 1% nano-SiO_2 addition became denser and less porous than that of other samples, and their compressive strength substantially increased. This could result in defective geopolymer structures because of the excessive dispersion of nano-SiO_2 in the mixture, resulting in a loose geopolymer structure with decreased compressive strength when 2% and 3% nano-SiO_2 was added.

4. Conclusions

A simple methodology using nano-SiO_2 and TFT-LCD waste glass with different ratios for producing a geopolymer material was successfully developed. The results obtained revealed that the setting time can be increased by adding TFT-LCD waste glass, and decreased by adding a large amount of nano-SiO_2. The waste glass-metakaolin-based geopolymer sample produced using 10% TFT-LCD waste glass together with the optimal amount of nano-SiO_2 (1%) exhibited the smallest cumulative pore volume and the highest compressive strength. The compressive strength of the geopolymer also increased with an increase in the curing time.

Moreover, the FTIR spectrum of the geopolymer product exhibited a distinct intensity band between 1300 and 900 cm^{-1}, which can be associated with the Si-O-T asymmetric vibration. This bond has been often used to determine the degree of polymerization of geopolymers. All geopolymer samples were compacted in the presence of the nano-SiO_2 activator, as shown in the microstructural analysis. Generally, applying nano-SiO_2 to fabricate a geopolymer material can result in a product with high uniformity, high compactness, and high compressive strength. Furthermore, TFT-LCD waste glass can be used to partially substitute metakaolin in the geopolymer, considerably decreasing the cost of the product.

Acknowledgements

The authors would like to thank the National Science Council of the Republic of China, Taiwan, for financially supporting this research under Contract No. NSC 99-2622-E-197-003-CC and 101-2923-I-011-001-MY4.

References

Alaa M.R., (2013), Metakaolin as cementitious material: History, scours, production and composition - A comprehensive overview, *Construction and Building Materials*, **41**, 303-318.

Álvarez-Ayuso E., Querol X., Plana F., Alastuey A., Moreno N., Izquierdo M., Font O., Moreno T., Diez S., Vázquez E., Barra M., (2008), Environmental, physical and structural characterisation of geopolymer matrixes synthesised from coal (co-)combustion fly ashes, *Journal of Hazardous Materials*, **154**, 175-183.

Amato A., Rocchetti L., Beolchini F., (2017), Evaluation of different strategies for end-of-life liquid crystal displays (LCD) management, *Environmental Engineering and Management Journal*, **16**, 1651-1657.

Andini S., Cioffi R., Colangelo F., Grieco T., Montagnaro F., Santoro L., (2008), Coal fly ash as raw material for the manufacture of geopolymer-based products, *Waste Management*, **28**, 416-423.

Chindaprasirt P., Jaturapitakkul C., Chalee W., Rattanasak U., (2009), Comparative study on the characteristics of fly ash and bottom ash geopolymers, *Waste Management*, **29**, 539 -543.

Davidovits J., (1989), Geopolymers and geopolymeric materials, *Journal of Thermal Analysis*, **35**, 429-441.

Davidovits J., (1991), Geopolymers: inorganic polymeric new materials, *Journal of Thermal Analysis*, **37**, 1633-1656.

Display Search, (2013), Growth Slowing for TFT LCD Glass Substrate Capacity, According to NPD DisplaySearch, On line at http://www.displaysearch.com.

Duxson P., Fernández-Jiménez A., Provis J.L., Lukey G.C., Palomo A., van Deventer J.S.J., (2007), Geopolymer technology: the current state of the art, *Journal of Materials Science*, **42**, 2917-2933.

Gao K., Lin K.L., Wang D.Y., Hwang C.L., Shiu H.S., Cheng T.W., (2014), Effects SiO_2/Na_2O molar ratio on mechanical properties and the microstructure of nano-SiO_2 metakaolin-based geopolymers, *Construction and Building Materials*, **53**, 503-510.

Granizo M.L., Blanco-Varela M.T., Palomo A., (2000), Influence of the starting kaolin on alkali-activated materials based on metakaolin. Study of the reaction parameters by isothermal conduction calorimetry, *Journal of Materials Science*, **35**, 6309-6315.

Heah C.Y., Kamarudin H., Mustafa Al Bakri A.M., Bnhussain M., Luqman M., Khairul Nizar I., Ruzaidi C.M., Liew Y.M., (2012), Study on solids-to-liquid and alkaline activator ratios on kaolin-based geopolymers, *Construction and Building Materials*, **35**, 912-922.

Khale D., Chaudhary R., (2007), Mechanism of geopolymerization and factors influencing its development: a review, *Journal of Materials Science*, **42**, 729-746.

Komnitsas K.A., (2011), Potential of geopolymer technology towards green buildings and sustainable cities, *Procedia Engineering*, **21**, 1023-1032.

Kong D.L.Y., Sanjayan J.G., Sagoe-Crentsil K., (2007), Comparative performance of geopolymers made with metakaolin and fly ash after exposure to elevated temperatures, *Cement and Concrete Research*, **37**, 1583-1589.

Lin K.L., (2007a), The effect of heating temperature of thin film transistor-liquid crystal display (TFT-LCD) electric-optical waste glass substitute partial clay as eco-brick, *Journal of Cleaner Production*, **15**, 1755-1759.

Lin K.L., (2007b), Use of thin film transistor liquid crystal display (TFT-LCD) waste glass in the production of ceramic tiles, *Journal of Hazardous Materials*, **148**, 91-97.

Lin K.L., Chang W.C., Lin D.F., Luo H.L., Tsai M.C., (2008), Effects of nano-SiO_2 and different ash particle sizes on sludge ash-cement mortar, *Journal of Environmental Management*, **88**, 708-714.

Lin K.L., Chang W.K., Chang T.C., Lee C.H., Lin C.H., (2009), Recycling thin film transistor liquid crystal display (TFT-LCD) waste glass produced as glass–ceramics, *Journal of Cleaner Production*, **17**, 1499-1503.

Lin K.L., Shiu H.S., Shie J.L., Cheng T.W., Hwang C.L., (2012), Effect of composition on characteristics of thin film transistor liquid crystal display (TFT-LCD) waste glass-metakaolin-based geopolymers, *Construction and Building Materials*, **36**, 501-507.

Park S.B., Lee B.C., Kim J.H., (2004), Studies on mechanical properties of concrete containing waste glass aggregate, *Cement and Concrete Research*, **34**, 2181-2189.

Popovici A., Popiţa G.E., Corbu O., Rusu T., Roşu C., Proorocu M., Smical I., (2015), Unconventional mortars with recycled cathode ray tubes waste glass, *Environmental Engineering and Management Journal*, **14**, 2661-2670.

Rodríguez E.D., Bernal S.A., Provis J.L., Paya J., Monzo J.M., Borrachero M.V., (2013), Effect of nanosilica-based activators on the performance of an alkali-activated fly ash binder, *Cement and Concrete Composites*, **35**, 1-11.

van Jaarsveld J.G.S., van Deventer J.S.J., Lorenzen L., (1997), The potential use of geopolymeric materials to immobilise toxic metals: part I. Theory and applications, *Minerals Engineering*, **10**, 659-669.

Wang H.Y., (2009), A study of the engineering properties of waste LCD glass applied to controlled low strength materials concrete, *Construction and Building Materials*, **23**, 2127-2131.

Wang H.Y., (2011), The effect of the proportion of thin film transistor-liquid crystal display (TFT-LCD) optical waste glass as a partial substitute for cement in cement mortar, *Construction and Building Materials*, **25**, 791-797.

Wang H.Y., Huang W.L., (2010), Durability of self-consolidating concrete using waste LCD glass, *Construction and Building Materials*, **24**, 1008-1013.

Wang W.J., Zhu X.R., Fang P.F., (2005), Analysis on reinforcement mechanism of nanometer silica fume reinforced cemented clay, *Journal of Zhejiang University Science*, **39**, 148-153.

Xu H., van Deventer J.S.J., (2000), The geopolymerization of alumino-silicate minerals, *International Journal of Mineral Processing*, **35**, 1688-1697.

Yang F.S., Zhou A.N., Ge L.M., Li T.L., Qu J.L., (2001), Nano technology in polymer modification applications, *Chemical Progress*, **20**, 9-12.

Zaharaki D., Komnitsas K., Perdikatsis V., (2010), Use of analytical techniques for identification of inorganic polymer gel composition, *Journal of Materials Science*, **45**, 2715-2724.

Zhang M.H., Islam J., Peethamparan S., (2012), Use of nano-silica to increase early strength and reduce setting time of concretes with high volumes of slag, *Cement and Concrete Composites*, **34**, 650-662.

Zhang Y., Sun W., Li Z., (2010), Composition design and microstructural characterization of calcined kaolin-based geopolymer cement, *Applied Clay Science*, **47**, 271-275.

Zheng Y., Xiong W., Liu W., Lei W., Yuan Q., (2005), Effect of nano addition on the microstructures and mechanical properties of Ti(C, N)-based cermets, *Ceramics International*, **31**, 165-170.